Bioengineering Adeno-Associated Viral Vectors for the Targeted Expression of Therapeutic Genes

A Thesis

Presented to the Faculty of
The School of Engineering and Applied Science
University of Virginia

In Partial Fulfillment
Of the Requirements for the Degree
Master of Science in Biomedical Engineering

Nathan A. Thomas
May 2014

This Thesis is submitted in partial fulfillment of the requirements for the degree of
Master of Science in Biomedical Engineering

_____
Author

This dissertation has been read and approved by the examining committee:

Brent A. French, Ph.D.
Dissertation Advisor

Jeffrey J. Saucerman, Ph.D.
Committee Chair

Victor E Laubach, Ph.D.

Accepted for the School of Engineering and Applied Science:

Dean, School of Engineering and Applied Science

May 2014

2

Acknowledgements

First off, I'd like to thank my advisor, Dr. Brent French, for endless help designing experiments and planning my project. I'd also like to thank my committee members, Dr. Jeff Saucerman, who had a lot of good suggestions along the way and is always thinking about future directions for projects, and Dr. Vic Laubach, who helped immensely with making my thesis clearer.

Enormous thanks goes to Dr. Bryan Piras, who helped me get my feet under me in the lab and taught me how to do 95% of the work that went into this thesis. He was also a great friend in lab and remains one outside of lab. I'd like to thank all of the current members of the French Lab, Alyssa Becker, Elie Chamaly, Lanlin Chen, and Sarah Hansen. Siva Dasa of the Kelley Lab was a big help whenever he could be as well. I'd also like to thank Renata Polanowska-Grabowska of the Saucerman Lab for isolating cardiomyocytes that made some of these experiments possible. Laura Woo of the Saucerman Lab has also been incredibly helpful with cardiomyocyte transfections and immunofluorescence experiments.

Last but definitely not least come the people who do not have a direct impact on the science I do, but keep me in the frame of mind required to keep working hard toward goals and to keep persevering when things aren't quite working out. I'd specifically like to acknowledge my parents, Brad and Stephanie, and my grandparents, who never fail to let me know how proud they are of me. Then there are the friends that have made life in Charlottesville more than just a daily grind. I won't list names because there would be too many to list, and in the small likelihood that any of them read this, they will know who they are. Thanks everyone.

Table of Contents

Abstract

Adeno-associated virus (AAV) vectors are increasingly used viral vectors for gene delivery in human gene therapy trials. They infect both nondividing and dividing cells and show long-term gene expression with low immunological response compared to other viral vectors used for gene therapy. Different AAV serotypes exhibit a variety of tissue tropisms and transduction efficiencies. A previous study in our lab has shown that serotype AAV9 is particularly effective for cardiac applications because of its uniform gene expression throughout the myocardium as well as its short lag phase, 2-3 weeks, to maximum gene expression. Furthermore, ischemia and reperfusion to the heart creates an environment that is more conducive to AAV9 transduction than healthy myocardium. In this study, I describe the engineering and evaluation of plasmids designed for packaging into AAV9 for cardiac-targeted gene therapy. I show that a plasmid with a bicistronic expression cassette containing neuregulin-1β (Nrg-1β) and green fluorescent protein (GFP) causes dual overexpression of these genes in vitro. I also show that the Nrg-1β is a functional protein via a proliferation assay with MCF7 breast cancer cells in vitro. This bicistronic cassette has been incorporated into multiple plasmid constructs driven by the promiscuous cytomegalovirus (CMV) promoter or the tissue-specific cardiac troponin-T (cTnT) promoter and flanked by two AAV inverted terminal repeats (ITR) for packaging into the AAV9 capsid for in vivo studies of its therapeutic potential.

List of Figures

Figure 1. Expression cassettes of plasmids used. A) pAcTnTNrgIRESeGFP carrying the cTnT promoter driving Nrg-1β, IRES, and GFP with miR-122 sites and a synthetic polyadenylation sequence. B) pACMVNrgIRESeGFP with Nrg-1β, IRES, and GFP driven from the CMV promoter. The 3' end of this cassette contains the SV40 polyadenylation sequence. C) pAcTnTNrgHA carries an HA-tagged Nrg-1β, IRES, and GFP driven from the cTnT promoter. D) pACMVNrgHA carries an HA-tagged Nrg-1β, IRES, and GFP driven from the CMV promoter.

Figure 2. mRNA analysis of AAV-293 cells transfected with pAcTnTNrgIRESeGFP or pAcTnTGFP and harvested three days post transfection. pAcTnTNrgIRESeGFP transfected cells show 31-fold more NRG-1β mRNA expression relative to pAcTnTGFP transfected cells. mRNA expression was normalized to GAPDH. (n=3/group, p<0.01)

Figure 3. mRNA analysis of AAV-293 cells transfected with pAcTnTNrgIRESeGFP or pAcTnTGFP and harvested three days post transfection. pAcTnTNrgIRESeGFP transfected cells show 36-fold more GFP mRNA expression relative to non-transfected cells. mRNA expression was normalized to GAPDH. (n=3/group, p<0.01)

Figure 4. Western blot analysis for expression of protein from pACMVNrgIRESeGFP and pACMVNrgHA. A) Lanes 1 and 2: 15 μg and 7.5 μg of AAV-293 whole cell lysate. Lanes 3 and 4: 15 μg and 10 μg of AAV-293 cells transfected with pACMVNrgIRESeGFP. Blot was incubated with rabbit polyclonal anti-Nrg primary antibody and goat anti-rabbit secondary. 4-20% polyacrylamide gel. B) Lane 1: 10 μg of AAV-293 whole cell lysate. Lanes 2 and 3: 20 μg and 10 μg of lysate from AAV-293 cells transfected with pACMVNrgHA. Blot was incubated with rabbit polyclonal anti-HA and goat polyclonal anti-GFP primary antibodies and donkey anti-rabbit 680 and donkey anti-goat 800 secondary antibodies. 12%polyacrylamide gel. GFP is in green and Nrg-1β is in red. The presence of similar band patterns around 90-110 kDa and 50-65 kDa in both blots with two different antibodies suggests that these bands are protein products of our plasmid.

Figure 5. Cell density of MCF7 cells after treatment with conditioned media + 1% FBS. Density was measured by absorbance reading of crystal violet uptake in cells. Compared to negative control, positive control and CMVNrgIRESeGFP-conditioned media show significantly higher cell density as measured by OD570 (n=3/group, p<0.05)

Figure 6. Cell density of MCF7 cells after treatment with conditioned media + 0.5% FBS. Density was measured by absorbance reading of crystal violet uptake in cells. Compared to negative control, CMVNrgIRESeGFP-conditioned media show significantly higher cell density as measured by OD570 (n=3/group, p<0.05)

Figure 7. Immunofluorescence of rat neonatal cardiomyocytes transfected with pAcTnTeGFP (A,B,C) or pAcTnTNrgHA (D,E,F). A) GFP fluorescence in pAcTnTGFP-transfected cardiomyocytes. B) Ki-67 and Nrg-1β staining shows Ki-67 positive nuclei but

no Nrg-1β (which stains the cell body) positive cells. C) Merged image of A and B plus dapi nuclear stain. D) GFP fluorescence in pAcTnTNrgHA-transfected cardiomyocytes. E) Ki-67 positive nuclei plus Nrg-1β positive cardiomyocytes. F) Merged image of D and E shows overlap of GFP+ and Nrg-1β+ cells, indicating coexpression of Nrg-1β and GFP.

Figure 8. mRNA analysis of AAV-293 cells transfected with pACMVApln, pAcTnTApln, or not transfected and harvested three days post transfection. pAcTnTApln transfected cells show 2800-fold more NRG-1β mRNA expression relative to cells that did not undergo transfection. mRNA expression was normalized to GAPDH. (n=3/group, p<0.01)

List of Abbreviations

AAV   adeno-associated virus
cTnT   cardiac Troponin-T
CMV   cytomegalovirus
Nrg-1β   neuregulin-1β
GFP   green fluorescent protein
ITR   inverted terminal repeat
MI   myocardial infarction
LV   left ventricular
ADAM   a disintegrin and metalloprotease
BACE1   β-site of myeloid precursor protein-cleaving enzyme
IRES   internal ribosome entry site
HA   hemaggluttinin
EMCV   encephalomyocarditis
APJ   angiotensin-like 1 receptor

Introduction:

LV Remodeling: Heart disease is the single leading cause of death in the United States. This year, an estimated 620,000 Americans will have their first myocardial infarction (MI) and around 295,000 will have a recurrent attack.[1] Heart failure following MI is a major cause of mortality and approximately 34% of the people who experience MI will ultimately die from it. Within the first few hours following MI, the heart begins a complex process of cardiac remodeling which may be defined as "molecular, cellular and interstitial changes that are manifested clinically as changes in size, shape and function of the heart after cardiac injury."[2] Left ventricular (LV) end-systolic volume is the major determinant of clinical outcome after recovery from MI, and is a function of the original infarct size.[3] It follows that therapies to improve cardiac outcome following MI should aim to reduce infarct size and limit LV remodeling.

The first mechanism behind LV remodeling is infarct expansion, a radial thinning and circumferential increase in the extent of a transmural infarct that occurs following acute MI.[4] During infarct expansion, infarcted myocardium is converted into mature scar. Following infarct expansion, the region of viable tissue immediately adjacent to the infarct, known as the infarct borderzone, plays a critical role in LV remodeling for weeks to months. Increased wall stress as well as neurohormonal and cytokine signaling may cause cardiomyocyte loss in the borderzone and cause a progressive increase in infarct size known as infarct extension.[5] Preventing the progressive loss of borderzone cardiomyocytes or reversing this aspect of the remodeling process has the potential to significantly improve left ventricular function following MI.

Cardiac Regeneration Strategies: The heart is one of the least regenerative organs in the body and until recently the paradigm of the adult human heart as a terminally differentiated organ went unchallenged.[6,7] However, in past 15 years, studies have discovered that cardiomyocytes do retain some proliferative capacity and that the adult heart may contain endogenous progenitor cells.[8,9] Despite the encouragement that cardiomyocytes do have endogenous regenerative mechanisms, current pharmacological, interventional, and operative therapies are limited in their ability to prevent heart failure following MI primarily because these therapies do not address the depletion of cardiomyocytes in the post-infarct heart.[10] Therapies aimed at overcoming this clinical deficiency using cell based therapy, tissue engineering, or reprogramming resident cells in the heart are beginning to emerge. This thesis outlines the beginning stages of two potential therapies intended to regenerate functional myocardium. The first strategy is to prevent cardiomyocyte cell death and induce proliferation in the borderzone after MI by programming the expression of Neuregulin-1β (Nrg-1β) in borderzone cardiomyocytes. The second strategy is to prevent cardiomyocyte death, improve pump function, and stimulate angiogenesis in the left ventricle by delivering apelin to borderzone cardiomyocytes. Accomplishing these strategies requires a vector that can target the heart and deliver the therapeutic gene in a time frame relevant to the prevention of LV remodeling.

Adeno-Associated Viral Vectors: As LV remodeling begins shortly after MI and subsides as early as two weeks after reperfusion in small animals, early intervention is necessary to protect the heart after infarct.[11] Gene therapy interventions to reduce the extent of LV

remodeling should ideally target at-risk cardiomyocytes and show rapid onset of gene expression.[12]

Adeno-associated virus (AAV) vectors are increasingly used as gene delivery vehicles in human trials of gene therapy.[13] They infect both nondividing and dividing cells and show long-term gene expression with low immunological response compared to other viral vectors used for gene therapy.[14] To date, 12 different AAV serotypes have been isolated from humans and over 100 from non-human primates.[13] These serotypes differ in their capsid shells which interact specifically with cell surface receptors. As a result, different serotypes exhibit a variety of tissue tropisms and transduction efficiencies.[15,16]

While AAV2 has been the most widely studied serotype to date, its lag phase of 4-6 weeks before reaching maximum gene expression in the heart limits its potential as a LV remodeling therapeutic vector.[17] Serotypes AAV6, AAV8, and AAV9 are better candidates because when delivered systemically they preferentially transduce cardiomyocytes and show uniform gene expression throughout the myocardium. Furthermore, they show a more rapid onset of gene expression and can reach maximum expression within 2-3 weeks.[18] A study published by our lab has also shown that ischemia and reperfusion to the heart creates an environment that is more conducive to AAV9 transduction than healthy myocardium.[12] This makes AAV9 an excellent gene delivery vector for cardiac therapies following MI.

Neuregulin-1:

Introduction: Neuregulin-1 (Nrg-1) was originally discovered in 1992 by researchers looking for the ligand for the ErbB2 transmembrane tyrosine kinase, whose overexpression is correlated with a number of human cancers.[19] Its critical role in cardiovascular signaling was not discovered until studies showed that mice with disrupted ErbB2, ErbB4, or Nrg-1 expression die between days 9 to 11 in utero due to failure in cardiac development.[20,21,22]

Nrg-1 is one of 4 structurally related genes (Nrg-1, Nrg-2, Nrg-3, and Nrg-4) encoding neuregulins, with Nrg-1 being the most abundant in the heart.[23] The Nrg-1 gene generates six types of proteins (I-VI) characterized by their N-terminal regions.[24] Alternative splicing of the gene results in at least 31 isoforms, all of which share a common EGF domain essential for receptor activation.[24,25] Receptor affinity is determined by alternative splicing at the C-terminal of the EGF domain, which results in either the α- or β-variant. In the adult heart, the β isoforms are 10 to 100 times more bioactive and show a higher affinity for ErbB3 and ErbB4 receptors.[26]

Most Nrg-1 isoforms are membrane bound proproteins that include a hydrophobic transmembrane domain and a cytoplasmic tail. In type I Nrg-1β, mature protein is released following proteolytic cleavage in the extracellular region on the C-terminal side of the EGF domain.[25] This cleavage is catalyzed by one of several a disintegrin and metalloproteases (ADAM) and β-site of amyloid precursor protein-cleaving enzyme (BACE1).[27,28] Following cleavage, the mature protein exerts its effects in a paracrine manner on ErbB tyrosine kinase receptors.

In the adult heart, NRG-1β is expressed on cardiac microvascular endothelial cells. Adult ventricular myocytes express ErbB1, ErbB2, and ErbB3, and numerous cellular

processes appear to be regulated by Nrg-1/ErbB signaling.[26] These processes include cell growth and survival, organization of myofilaments, angiogenesis, and cardiomyocyte proliferation.[29,30,31,32] Recent studies have demonstrated that recombinant Nrg-1β can induce adult cardiomyocytes to proliferate in mice and that Nrg-1β delivery can improve cardiac function in rats following MI.[33,34,35,36] However, these studies have relied either on administration of recombinant proteins which have a short half-life in the blood, lentiviral vectors which are quickly inactivated by complement, or direct injection into the myocardium which is not clinically practical. A more clinically feasible approach would be a vector that can be injected systemically, elicits minimal immune responses, and can specifically target cardiomyocytes. In the following sections, I describe the design and initial evaluation of an AAV9 vector to deliver Nrg-1β to borderzone cardiomyocytes.

Materials and Methods

Cell Culture: AAV-293 cell line (Agilent Technologies Inc., Clara, CA) was cultured in DMEM with 7% FBS, 1% penicillin-streptomycin, and glutamate. MCF7 breast cancer cell line (a gift from the Bouton Lab) was cultured in DMEM with 10% FBS and 1% penicillin-streptomycin. Both cell lines were maintained at 37°C in a humidified atmosphere of 5% CO_2.

Plasmid Design: cDNA for NRG-β1 was purchased from Sino Biological (Beijing, China) and was PCR amplified to add an EcoRI site 5' and a BamHI site 3' of the coding sequence. Phusion high-fidelity master mix (Thermo Scientific, Waltham, MA) was used for PCR to avoid amplification errors. Plasmid pAAV-CMV-luc-IRES-GFP (Penn Vector Core, Philadelphia, PA) was digested with BamHI and NotI to remove a 1,327 base pair sequence containing the encephalomyocarditis virus internal ribosome entry site (IRES) and eGFP.

14

The IRES allows for a bicistronic vector, or a vector that translates two proteins separately from the same RNA transcript. Use of the IRES in this vector allows us to deliver Nrg-1β as a therapeutic gene while also using eGFP as a reporter gene to visualize which cells were effectively transduced.

The amplified Nrg-1β and the 1,327 base pair sequence were inserted by triple ligation into a plasmid backbone containing the AAV2 ITRs and cardiac Troponin T (cTnT) promoter. This promoter is used to limit gene expression from these plasmids to cardiomyocytes. An oligonucleotide with a NotI site 5' and a KpnI site 3' of three miRNA-122 target sites as well as an oligonucleotide containing a minimal poly-adenylation sequence flanked by a KpnI site 3' and SalI site 5' were purchased from Integrated DNA Technologies (Coralville, IA). miRNA-122 target sites are used to destabilize the plasmid in the liver where miRNA-122 is expressed abundantly. The minimal poly-adenylation sequence was used instead of the more common SV40 polyadenylation sequence in order to keep the construct size small. Sense and antisense oligonucleotides were annealed and triple ligated into the plasmid containing the cTnT promoter, NRG-1β, IRES, and eGFP. The new plasmid, pAcTnTNrgIRESeGFP was sequenced to confirm proper cloning.

To add an optimal consensus sequence to pAcTnTNrgIRESeGFP, a forward primer containing the Kozak sequence (5'-GCTACCATGGGCCGCCACCATGTCCGAGCGCAAAGAAGGCAG-3') was purchased and used to amplify the Nrg-1β cDNA. The amplified sequence was inserted into pAcTnTNrgIRESeGFP in place of the current Nrg-1β sequence. This plasmid was sequenced to check for errors in the nucleotide sequence.

To create a plasmid with the CMV promoter driving Nrg-1β, a 2,188 base pair fragment was released from pAcTnTNrgIRESeGFP with HindIII and ligated into two HindIII sites in pAAV-CMV-luc-IRES-eGFP to create pACMVNrgIRESeGFP.

pAcTnTNrgHA was created by replacing the 3' end of the expression cassette in pAcTnTNrgIRESeGFP containing the mir-122 target sites and minimal polyadenylation sequence with the SV40 polyadenylation sequence. An influenza hemaggluttinin (HA) epitope tag was cloned onto the C-terminal of the Nrg-1β cDNA by PCR amplification using primers 5'-GCTACCATGGGCCGCCACCATGTCCGAGCGCAAAGAAGGCAG-3' (Forward) and 5'-GCTAGGATCCTTAAGCGTAGTCTGGGACGTCGTATGGGTATACAGCAATA-3' (Reverse). The amplified product was digested with EcoRI and BamHI and ligated into the backbone containing AAV2 ITRs, cTnT promoter, IRES, eGFP and SV40 polyA sequence. The amplified product was also ligated into the EcoRI and BamHI sites in pACMVNrgIRESeGFP to make pACMVNrgHA. See Figure 1 for a diagram of important plasmids.
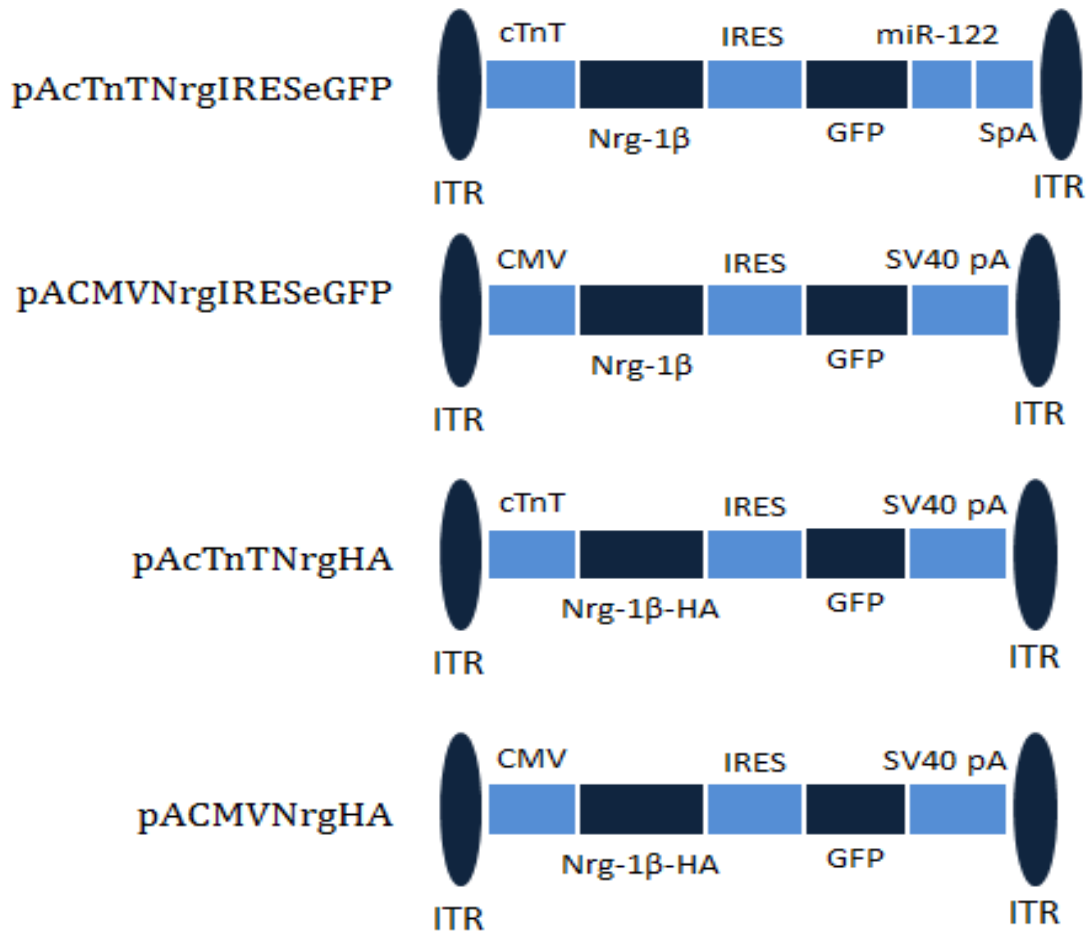
Figure 1. Expression cassettes of plasmids used. A) pAcTnTNrgIRESeGFP carrying the cTnT promoter carrying Nrg-1β, IRES, and GFP with miR-122 sites and a synthetic polyadenylation sequence. B) pACMVNrgIRESeGFP with Nrg-1β, IRES, and GFP driven from the CMV promoter. The 3' end of this cassette contains the SV40 polyadenylation sequence. C) pAcTnTNrgHA carries an HA-tagged Nrg-1β, IRES, and GFP driven from the cTnT promoter. D) pACMVNrgHA carries an HA-tagged Nrg-1β, IRES, and GFP driven from the CMV promoter.

In Vitro Transfection: In vitro transfections of the AAV-293 and MCF7 cell lines were performed using the calcium phosphate method.

AAV Vector Production: pAcTnTNrgIRESeGFP was packaged into AAV9 capsids with a calcium phosphate triple transfection of AAV-293 cells. AAV was then purified by ammonium sulfate fractionation and iodixanol gradient centrifugation. AAV titer [viral genomes (vg)/ml] was determined by qPCR. Known copy numbers ($10^5 - 10^9$) of

pAcTnTNrgIRESeGFP were used to construct the standard curve for quantification. The following primers were used to amplify GFP: 5'-TGACCCTGAAGTTCATCTGCACCA-3' (forward) and 5'-TCTTGTAGTTGCCGTCGTCCTTGA-3' (reverse). .

Animal Procedures: The animal protocol used in this study was approved by the University of Virginia Institutional Animal Care and Use Committee (Protocol Number: 2802) and strictly conformed to the "Guide for the Care and Use of Laboratory Animals" (NIH Publication 85-23, revised 1985).

Vector Administration: 12 week old C57/BL6 mice were anesthetized with 1-1.2% isofluorane in oxygen while a needle was inserted into the tail vein and viral doses of 4×10^{11} or 5×10^{11} viral genomes in PBS were injected.

Fluorescence Microscopy: Hearts were removed and fixed for one hour at room temperature in 4% PFA, rinsed in PBS, and incubated overnight at 4° in 30% sucrose before embedding in OCT. Six μm cryosections were cut from each tissue and imaged with an Olympus BX-41 Microscope (Olympus America, Inc., Center Valley, PA) with a Retiga-2000R camera (QImaging, Surrey, BC).

mRNA Analysis: For mRNA analysis in vitro, cultured cells were trypsinized, collected, pelleted, and RNA was isolated using the RNeasy Mini Kit (Qiagen, Inc., Valencia, CA). cDNA was synthesized using the iScript cDNA Synthesis Kit (Bio-Rad Laboratories, Hercules, CA). Relative amount of mRNA compared to control treatments was assessed using the Bio-Rad CFX96 Real-Time PCR Detection System and analyzed using the comparative C_T method normalized to GAPDH expression.

For mRNA analysis, whole hearts were removed and dissected into thirds. One third was stored in RNAlater (Qiagen Inc.) at -80°C until processing with the Qiagen AllPrep

DNA/RNA system. After isolating RNA, cDNA was synthesized with the Bio-Rad iScript cDNA Synthesis Kit and quantitative PCR was performed with Bio-Rad iTaq Universal SYBR Green Supermix.

The following primers were used for amplification: NRG-β1: 5'-CGTCATCTCCAGTGAGCATATT-3' (forward) and 5' – TAGGAGTCTGGGTGACAGTAG-3' (reverse), GFP: TGACCCTGAAGTTCATCTGCACCA-3' (forward) and 5'-TCTTGTAGTTGCCGTCGTCCTTGA-3' (reverse), GAPDH 5'-ACCCACTCCTCCACCTTTGAC-3' (forward) and 5'- TGTTGCTGTAGCCAAATTCGTT -3' (reverse)

Western Analysis: Isolated hearts were homogenized in buffer containing 50 mM Tris-HCL, 2 mM of EDTA and EGTA, 0.3% Triton-X 100, and Halt Protease Inhibitor Cocktail (Thermo Scientific, Rockford, IL). Total protein content was quantified using the DC Protein Assay from Bio-Rad. Equal amounts of protein were electrophoresed under reducing conditions on a polyacrylamide gel and then transferred onto polyvinylidene fluoride membranes. After blocking for one hour in 10% milk in TBS membranes were incubated overnight at 4°C with primary antibodies diluted in 5% milk in TBS with .01%SDS and 0.2% Tween-20. After washing membranes with TBS+0.1% Tween-20, they were incubated for one hour at room temperature with secondary antibody. Membranes were imaged with fluorescence on a Licor Odyssey Imaging System (Li-Cor Biosciences, Lincoln, NE).

Cells from culture were lysed and homogenized in RIPA buffer with Halt Protease Inhibitor Cocktail, and assessed for total protein content using the DC Protein Assay from Bio-Rad before immunoblotting according to the protocol above. Antibodies used for immunoblot experiments were: rabbit anti-NRG-β1 at 1:100 (SC-348, Santa Cruz

Biotechnology, Santa Cruz, CA), rabbit anti-HA at 1:2000 (Bethyl Laboratories, Montgomery, TX) goat anti-GFP at 1:3000 (BA-0702, Vector Laboratories, Inc., Burlingame, CA), chicken anti-alpha tubulin at 1:1000 (Sigma Aldrich, St. Louis, MO).

Cell Proliferation Assay: MCF7 cells were plated in 12-well culture dishes at a density of 50,000 cells/well in media containing 10% FBS and allowed to adhere for 24 hours. After 24 hours, media was replaced with a 1:2 dilution of conditioned media to fresh media containing 1% FBS. Cells were assessed for cell density at the time of media change and every 24 hours after.

To assess cell density, cells were washed 2x with PBS, fixed for 5 minutes with 4% paraformaldehyde in PBS, washed in dH_2O 2x and allowed to air dry in a sterile hood for one hour. After one hour, cells were incubated in 4% crystal violet in PBS for 30 minutes, washed 2x in dH_2O, and allowed to air dry for an hour. Methanol was added to the wells while shaking for 30 minutes to solubilize crystal violet. Wells were diluted 1:10 before measuring optical density of crystal violet solubilized in methanol at a wavelength of 570 nm with a spectrophotometer.

Immunofluorescence: Cardiomyocytes were isolated from neonatal rats and plated on 96-well plates (by Renata Polanowska-Grabowska). Transfections were performed using Lipofectamine 3000 (Life Technologies, Carlsbad, CA) by Laura Woo. Three days later, cells were fixed, blocked, and stained overnight with rabbit anti-Ki-67 and rabbit anti-Nrg-1β primary antibodies and Dapi. Following primary incubation, cells were incubated with anti-rabbit secondary antibody conjugated to Alexa Fluor 568.

Results:

NRG-1β and GFP mRNA are Overexpressed in Transfected 293 Cells: To verify that

plasmids could cause overexpression of the desired mRNA, AAV-293 cells were transfected

and mRNA was analyzed three days later. Figure 2 shows NRG-1β mRNA expression

relative to a control transfection with a plasmid expressing GFP from the cTnT promoter.

Compared to control transfection, cells transfected with pAcTnTNrgIRESeGFP express 31
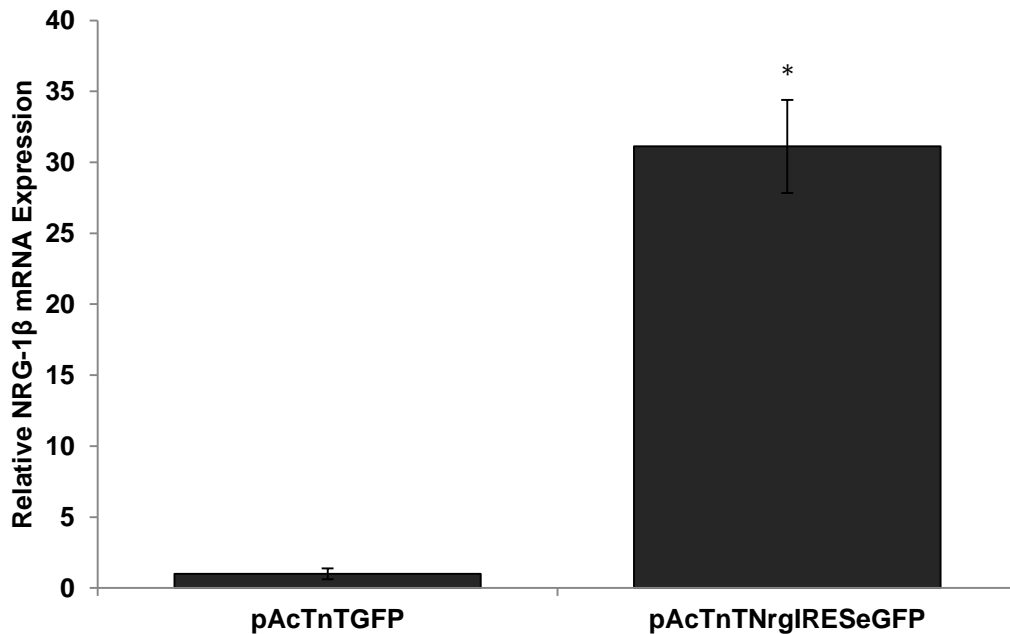
times more NRG-1β mRNA (n=3/group, p<0.01).

Figure 2. mRNA analysis of AAV-293 cells transfected with pAcTnTNrgIRESeGFP or pAcTnTGFP and harvested three days post transfection. pAcTnTNrgIRESeGFP transfected cells show 31-fold more NRG-1β mRNA expression relative to pAcTnTGFP transfected cells. mRNA expression was normalized to GAPDH. (n=3/group, p<0.01)

To determine how the IRES affected mRNA transcript levels, GFP mRNA expression

by cells transfected with pAcTnTGFP was compared to expression by cells transfected with

pAcTnTNrgIRESeGFP. GFP mRNA expression was almost three-fold weaker in the plasmid

with the IRES compared to GFP driven by the cTnT promoter. However, compared to PCR

background noise in cells that were not transfected, pAcTnTNrgIRESeGFP transfected cells had 36-fold more mRNA expression as determined by qPCR (Figure 3).
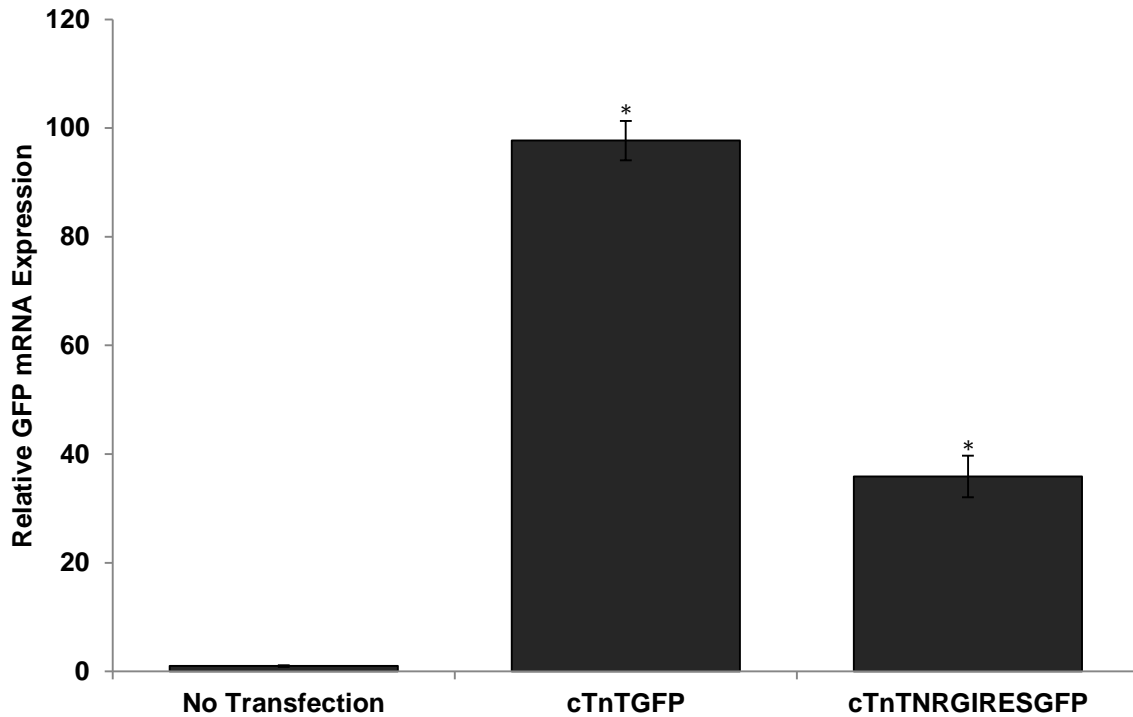

Figure 3. mRNA analysis of AAV-293 cells transfected with pAcTnTNrgIRESeGFP or pAcTnTGFP and harvested three days post transfection. pAcTnTNrgIRESeGFP transfected cells show 36-fold more GFP mRNA expression relative to non-transfected cells. mRNA expression was normalized to GAPDH. (n=3/group, p<0.01)

Pilot In Vivo Study Shows Minimal Neuregulin and GFP Overexpression: Once it was determined that pAcTnTNrgIRESeGFP could cause overexpression of NRG-1β and GFP mRNA in transfected cells in vitro, the plasmid was packaged into AAV9 capsid for a pilot study in vivo. Three C57/BL6 mice were given tail vein injections containing saline, 4×10^{11} viral genomes, or 5×10^{11} viral genomes (vg), corresponding to 0, 1.6×10^{13} and 2×10^{13} vg/kg body weight respectively. The dose chosen was based on previous studies with cardiac-targeted AAV9 in our lab. Three weeks after injection, mice were euthanized and hearts were analyzed for RNA and protein expression.

Compared to saline injected mice, mice injected with AAV9 showed a 45- and 71-fold increase in GFP mRNA, and a 65- and 30-fold increase in NRG-1β mRNA. However, after sectioning heart tissues for fluorescence microscopy, no GFP-positive cardiomyocytes were seen in heart sections. Upon Western blot analysis of excised hearts, NRG-1β protein expression level in AAV9 injected mice was similar to saline-injected control. GFP protein was not detected.

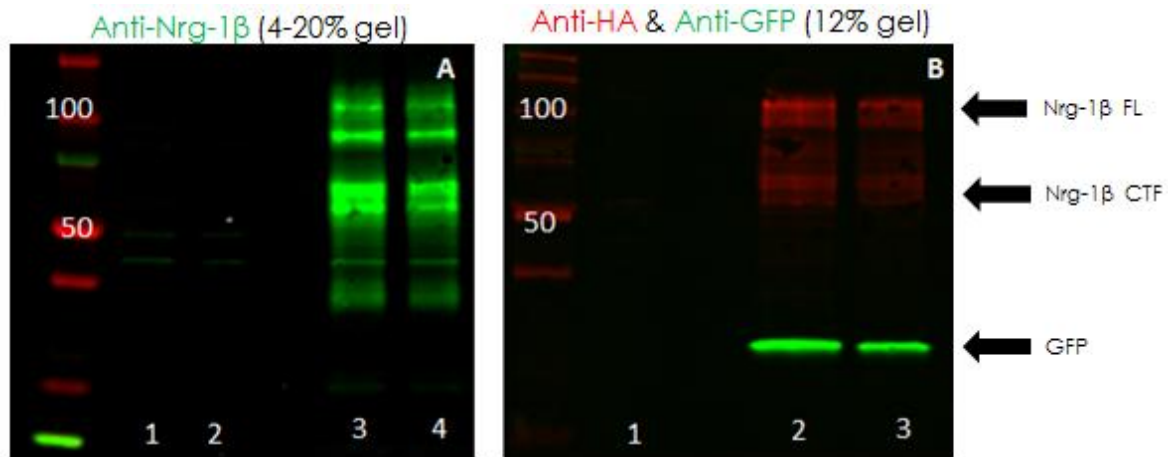**pACMVNrgHA and pAcTnTNrgHA Show Transcript and Protein Overexpression In Vitro:** To troubleshoot the low expression of protein seen from pAcTnTNrgIRESeGFP, new plasmids were designed. The strong, ubiquitous, human cytomegalovirus (CMV) enhancer and promoter was used to drive NRG-1β expression in pACMVNrgIRESeGFP. This plasmid also contains the IRES and GFP 3' of NRG-1β cDNA. The SV40 polyadenylation sequence is 3' of the GFP.

Because NRG-1β protein can be proteolytically cleaved in numerous ways, immunoblots of protein harvested from AAV-293 cells transfected with pAcTnTNrgIRESeGFP and pACMVNrgIRESeGFP showed multiple reactive bands when incubating with a primary antibody to the NRG-1β C-terminus (SC-348, Santa Cruz Biotechnology). Determining which reactive bands corresponded to the expression of protein from our plasmid construct proved especially difficult. To make interpretation easier, the human influenza hemagglutinin (HA) tag was cloned into the 3' end of the NRG-1β cDNA in existing plasmid constructs. Use of an HA tag allows for specific identification of proteins expressing that tag using an anti-HA antibody. pAcTnTNrgIRESeGFP was further modified to remove the minimal polyadenylation sequence and miRNA-122 target sites. This was in an effort to remove parts of the plasmid that may have been responsible for low

transcript and protein levels. Although nothing was found in a literature search, the possibility still exists that AAV-293 cells express miRNA-122. If so, much of the mRNA may have been degraded before translation. In the new construct, pAcTnTNrgHA, the SV40 polyadenylation sequence was inserted in place of the miRNA-122 target sites and the minimal polyadenylation sequence.

Compared with AAV-293 cells that did not undergo transfection, pACMVNrgIRESeGFP-transfected cells showed approximately a 5700-fold increase in NRG-1β mRNA level and 57000-fold increase in GFP mRNA as assessed by qPCR (n=3/group, p<0.01).

Western blot analysis of whole cell lysate of untreated AAV-293 cells, or cells transfected with pACMVNrgIRESeGFP, pACMVNrgHA was performed to verify that protein was being expressed from our cassette. Figure 4 shows two blots, one loaded with untreated AAV-293 cells or AAV-293 cells transfected with pACMVNrgIRESeGFP and incubated with primary antibody to the Nrg-1β C-terminus (SC348), the other loaded with untreated AAV-293 cells or AAV-293 cells transfected with pACMVNrgHA and incubated with anti-HA antibody. Both blots have similar band patterns, with bands in the 50-65 kDa and 90-110 kDa range that are not visible in untreated 293 controls. Because separate antibodies for Nrg-1β and HA-tag reacted with products that migrate at similar molecular weights, we conclude that these are proteins being expressed as a result of transfection with our cassette. In addition, Figure 4B shows GFP expression at its molecular weight of 27 kDa. Expression of GFP, the downstream gene in our bicistronic vector also strongly suggests that the gene in front of the IRES, Nrg-1β is being produced.

Figure 4. Western blot analysis for expression of protein from pACMVNrgIRESeGFP and pACMVNrgHA. A) Lanes 1 and 2: 15 µg and 7.5 µg of AAV-293 whole cell lysate. Lanes 3 and 4: 15 µg and 10 µg of AAV-293 cells transfected with pACMVNrgIRESeGPF. Blot was incubated with rabbit polyclonal anti-Nrg primary antibody and goat anti-rabbit secondary. 4-20% polyacrylamide gel. B) Lane 1: 10 µg of AAV-293 whole cell lysate. Lanes 2 and 3: 20 ug and 10 ug of lysate from AAV-293 cells transfected with pACMVNrgHA. Blot was incubated with rabbit polyclonal anti-HA and goat polyclonal anti-GFP primary antibodies and donkey anti-rabbit 680 and donkey anti-goat 800 secondary antibodies. 12%polyacrylamide gel. GFP is in green and Nrg-1β is in red. The presence of similar band patterns around 90-110 kDa and 50-65 kDa in both blots with two different antibodies suggests that these bands are protein products of our plasmid.

Conditioned Media from Cells Transfected with pACMVNrgHA causes Increased Proliferation in MCF-7 Cells: To assess the biological function of NRG-1β protein with the HA-tag, an in vitro proliferation assay was performed on the MCF7 breast cancer cell line. In this cell line, NRG-1β stimulation induces intracellular signaling via formation of ErbB2-ErbB3 heterodimers.[37]

MCF7 cells were treated with conditioned media from AAV-293 cells transfected with pAcTnTNrgHA, pACMVNrgHA, or pAcTnTGFP (negative control). This media was supplemented with either 1% (Figure 5) or 0.5% (Figure 6) FBS. Conditioned media from pAcTnTGFP-transfected AAV-293 cells supplemented with 10 ng/ml of recombinant human NRG-1β protein served as a positive control. Compared to negative control, media from the pACMVNrgHA-transfected cells caused cells to reach a higher density three days after addition of media (Figure 5, n=3/group, p<0.05). This result suggests that the HA-

tagged protein produced by cells transfected with our plasmids is biologically active and can induce proliferation of MCF7 cells beyond basal levels. Conditioned media from cells transfected with pAcTnTNrgHA did not cause proliferation above negative control.
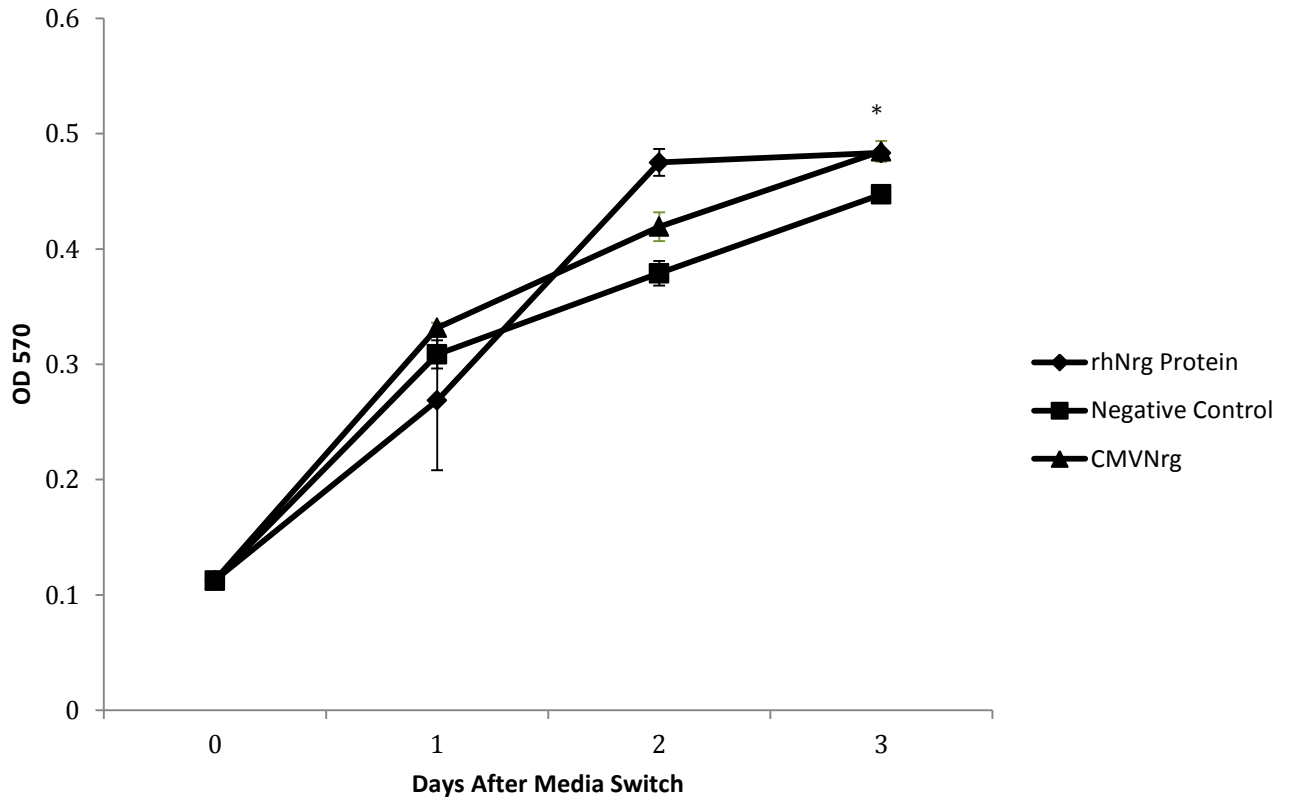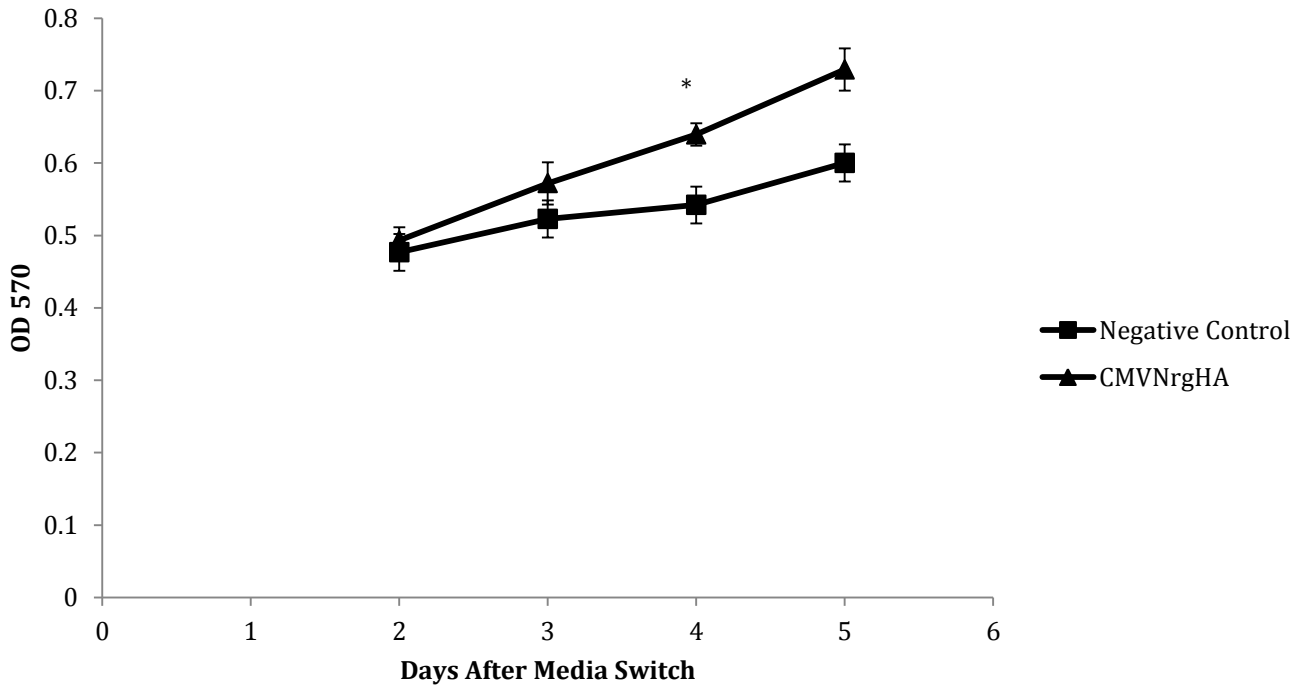

Figure 5. Cell density of MCF7 cells after treatment with conditioned media + 1% FBS. Density was measured by absorbance reading of crystal violet uptake in cells. Compared to negative control, positive control and CMVNrgIRESeGFP-conditioned media show significantly higher cell density as measured by OD570 (n=3/group, p<0.05)

As a second iteration of the proliferation assay, the percent of FBS in conditioned media was reduced in an attempt to lower baseline proliferation. Figure 6 shows the results of the second experiment. At day 4 after media switch, cell density is significantly higher in wells treated with conditioned media from pACMVNrgHA-transfected 293 cells. Cells in the control group in this experiment show less proliferation than the experiment with 1% FBS.

26

Figure 6. Cell density of MCF7 cells after treatment with conditioned media + 0.5% FBS. Density was measured by absorbance reading of crystal violet uptake in cells. Compared to negative control, CMVNrgIRESeGFP-conditioned media show significantly higher cell density as measured by OD570 (n=3/group, p<0.05)

Imunnofluorescence Shows Co-expression of Nrg-1β and GFP

To determine whether cardiomyocytes could co-express Nrg-1β and GFP, rat neonatal cardiomyocytes were isolated, plated, and transfected with pAcTnTGFP, pACMVNrgHA, or pAcTnTNrgHA. Transfections were performed by Laura Woo.

Cells transfected with pAcTnTGFP show GFP fluorescence but do not express Nrg-1β (Figure 7). Cells transfected with pAcTnTNrgHA express GFP as well as Nrg-1β. Similar co-expression of Nrg-1β and GFP was seen in cardiomyocytes transfected with pACMVNrgHA. The absence of Nrg-1β in cardiomyocytes transfected with plasmids not containing the cDNA for the Nrg-1β and the presence of Nrg-1β and GFP in cells transfected with plasmids

27

containing Nrg-1β cDNA and the GFP gene suggests that our plasmids can cause

cardiomyocytes to co-express Nrg-1β and GFP.
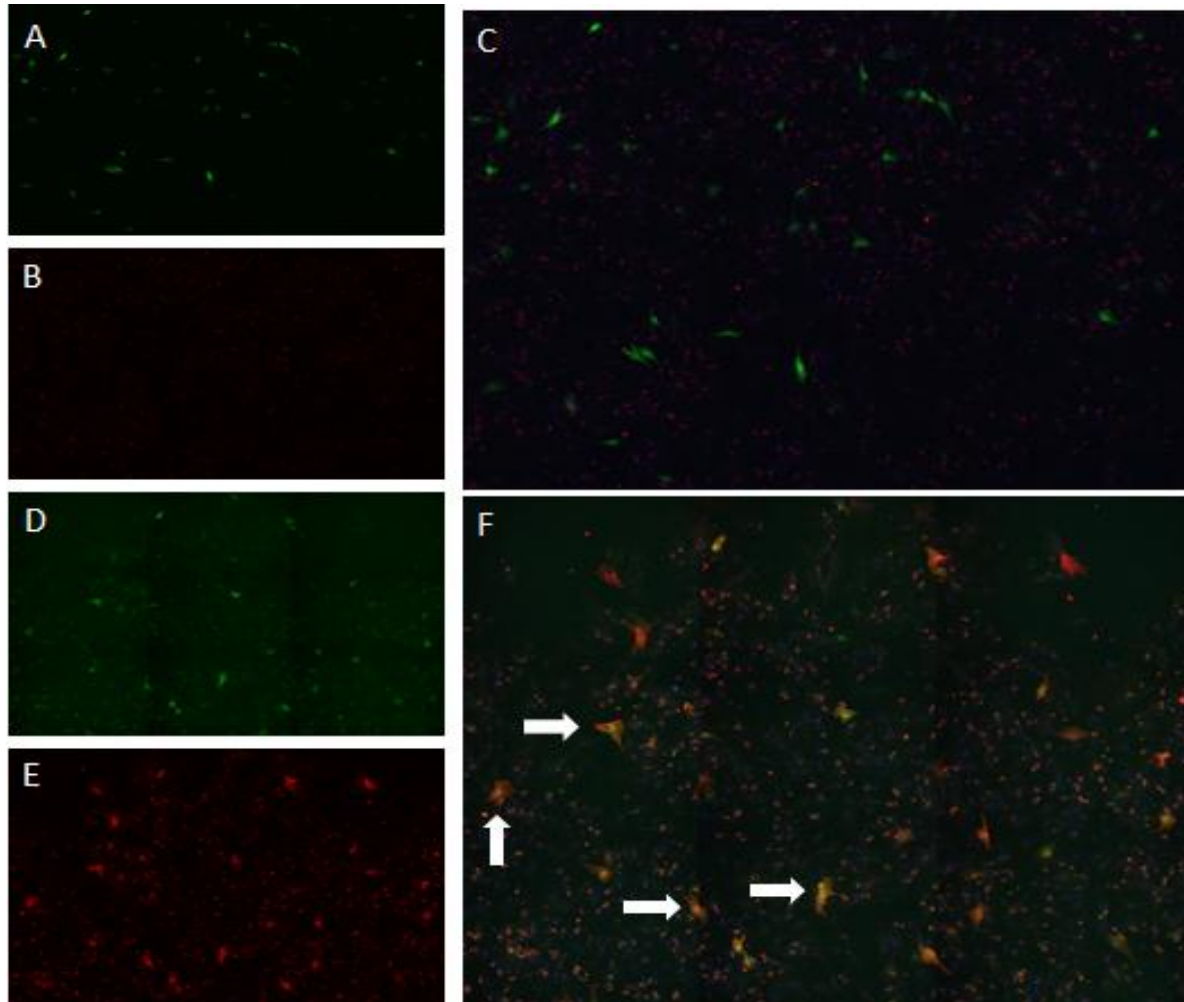
Figure 7. Immunofluorescence of rat neonatal cardiomyocytes transfected with pAcTnTeGFP (A,B,C) or pAcTnTNrgHA (D,E,F). A) GFP fluorescence in pAcTnTGFP- transfected cardiomyocytes. B) Ki-67 and Nrg-1β staining shows Ki-67 positive nuclei but no Nrg-1β (which stains the cell body) positive cells. C) Merged image of A and B plus dapi nuclear stain. D) GFP fluorescence in pAcTnTNrgHA-transfected cardiomyocytes. E) Ki-67 positive nuclei plus Nrg-1β positive cardiomyocytes. F) Merged image of D and E shows overlap of GFP+ and Nrg-1β+ cells, indicating coexpression of Nrg-1β and GFP.

Discussion: In the previous sections, I have described two iterations of an expression

cassette containing NRG-1β cDNA and GFP flanked by AAV2 ITRs and driven by the cTnT

promoter. In addition, I have described the creation and testing of a plasmid with the same

expression cassette driven by the strong, ubiquitous, CMV promoter. While the first

iteration of the cassette did not fare well in our pilot study, there are a number of reasons this may have been the case. First, in an attempt to keep the expression cassette small to facilitate large therapeutic genes in the future, this plasmid made use of a synthetic polyadenylation sequence only 49 base pairs long reported by Levitt et al.[38] Our lab has never tested this polyadenylation sequence previously. Therefore, we are unsure of its impact on transcript stability, nuclear export, and translation to protein – processes in which an efficient polyadenylation sequence is important for.

Furthermore, although the lab has tested the effect of miRNA-122 target sites on protein expression in vivo, in vitro analysis of their effect on protein expression in AAV-293 cells has not been tested. As a result, in vitro analysis of the pAcTnTNrgIRESeGFP plasmid was difficult because we were unsure of the extent to which miRNA-122 target sites may have been limiting protein expression.

This was also the first time our lab has worked with an IRES for bicistronic protein expression. Reports on the efficiency of gene expression from the EMCV IRES vary, but expression of the gene behind the IRES is not expected to be as strong as the first gene in a bicistronic vector. Again, the inability to quantify the effect that this had on GFP expression made in vitro analysis difficult. IRES activity is also cell-type specific, and its activity level in AAV-293 cells compared to murine cardiomyocytes is unknown.

Despite the difficulties with the first iteration of the cTnT driven plasmid, recent results have been more promising. I have shown that AAV-293 cells transfected with pACMVNrgHA plasmid overexpress NRG-1β compared to non-transfected AAV-293 cells. The immunoreactive band common to immunoblots stained with both anti-NRG-1β and anti-HA is the protein product resulting from transfection with my engineered expression

cassette. In addition, the NRG-1β protein translated as a result of transfection with pACMVNrgHA is functional as evidenced by the ability to cause increased MCF7 proliferation in vitro compared to control. As the cDNA is the same, this also implies that protein from pAcTnTNrgHA plasmid would be functional as well. Concentration in conditioned media may not have been high enough to induce proliferation above basal levels.

Finally, I have shown with immunofluorescence that cardiomyocytes transfected with my plasmids pAcTnTNrgHA and pACMVNrgHA co-express NRG-1β and GFP. In light of these results, I believe another pilot study in vivo is warranted. Further work is required to elucidate the reasons behind the low protein expression witnessed in experiments with the first iteration of the pAcTnTNrgIRESeGFP plasmid.

Apelin:

Introduction: In 1998, the endogenous ligand for the "orphan" angiotensin-like 1 (APJ) receptor was isolated from bovine stomach extracts.[39] The ligand, apelin, is a 77 amino acid pre-protein that is cleaved to become one of several active peptides of differing length.[40] Apelin and its receptor, APJ, mRNA are found in tissues throughout the body, including particularly high levels in the cerebellum, vascular endothelium, heart, lung, and kidney. In humans, APJ is expressed on cardiomyocytes, vascular smooth muscle cells, and vascular and endocardial endothelial cells.[41]

Apelin has been implicated in a number of functions that include glucose metabolism, fluid balance, and thermoregulation but the most widely studied role to date has been regulating cardiovascular homeostasis.[42] Bolus injection of apelin in rats causes a rapid fall in mean arterial pressure mediated by the APJ receptor and eNOS activation.[43] At the same time, apelin can stimulate myosin-light chain phosphorylation in mouse and rat vascular smooth muscle, suggesting that apelin can also induce contraction. However, apelin is considered a potent vasodilator because smooth muscular contraction is outweighed by vasodilation through stimulation of nitric oxide production when endothelium is intact.[42]

Numerous effects of apelin on the heart have been reported. In humans, myocardial expression of apelin and APJ are downregulated in patients with severe heart failure and plasma apelin levels are significantly reduced.[44,45] In isolated rat hearts, apelin increases cardiac contractility.[46] In mice after MI, apelin injected into ischemic myocardium can recruit bone-marrow derived cells to the heart to promote neovascularization, diminish infarct size, and improve cardiac function.[47] Intraperitoneal injection of apelin also reduces

LV preload and afterload without resulting in cardiac hypertrophy.[48] While more work is needed to further elucidate the mechanisms behind these characteristics of apelin, the functional improvement of the heart in response to apelin is reason to imagine a therapeutic potential for the treatment of heart failure. The following section describes the design and functional testing of a plasmid for packaging into AAV9 for upregulation of apelin post-MI.

Materials and Methods

Cell Culture: AAV293 cells were cultured in DMEM with 7% FBS, 1% penicillin-streptomycin, and .6% glutamate. bEND.3 brain endothelial cell line(a gift from the Lawrence Lab) was cultured in DMEM with 10% FBS and 1% penicillin-streptomycin. Both cell lines were maintained at 37°C in a humidified atmosphere of 5% CO_2.

Plasmid Design: Apelin cDNA in an expression vector containing the CMV promoter (pACMVApln) was purchased from Transomic Technologies (Huntsville, AL). A 768 base pair portion containing the coding sequence of the cDNA was restriction digested using KpnI and BamHI and inserted by ligation into a plasmid containing AAV2 ITRs and the cardiac troponin T (cTnT) promoter. The new plasmid, pAcTnTApln was sequenced to confirm that the cloning was accurate.

In Vitro Transfection: In vitro transfections of the AAV-293 (Agilent Technologies Inc., Clara, CA) and MCF7 (a gift from Dr. Bouton) cell lines were performed using the calcium phosphate method.

mRNA Analysis: For mRNA analysis in vitro, cultured cells were trypsinized, collected, pelleted, and RNA was isolated using the RNeasy Mini Kit (Qiagen, Inc., Valencia, CA). cDNA was synthesized using the iScript cDNA Synthesis Kit (Bio-Rad Laboratories, Hercules, CA).

Relative amount of mRNA compared to control treatments was assessed using the Bio-Rad CFX96 Real-Time PCR Detection System and analyzed using the comparative C_T method normalized to GAPDH expression.

Cell Proliferation Assay: bEND.3 cells were plated in 12-well culture dishes at a density of 50,000 cells/well in media containing 1% FBS and allowed to adhere for 24 hours. After 24 hours, cells were treated with filtered conditioned media from 293 cells transfected with plasmids containing either the pAcTnTGFP (negative control), pACMVApln, or pAcTnTApln cassettes.

To assess proliferation, cells were washed 2x with PBS, fixed for 5 minutes with 4% paraformaldehyde in PBS, washed in dH_2O 2x and allowed to air dry in a sterile hood for one hour. After one hour, cells were incubated in 4% crystal violet in PBS for 30 minutes, washed 2x in dH_2O, and allowed to air dry for an hour. Methanol was added to the wells while shaking for 30 minutes to solubilize crystal violet. Wells were diluted 1:10 before measuring optical density at a wavelength of 570 nm with a spectrophotometer.

Results:

pAcTnTApln Causes Overexpression of Apelin In Vitro: AAV-293 cells were transfected in vitro with plasmids containing apelin cDNA expressed from either the CMV promoter or the cTnT promoter. After mRNA analysis by qPCR, apelin driven by the CMV promoter showed a 22,000 fold increase in mRNA expression, while apelin driven by the cTnT promoter showed a 2800-fold increase vs. control (Figure 8, n=3/group, p<0.01)
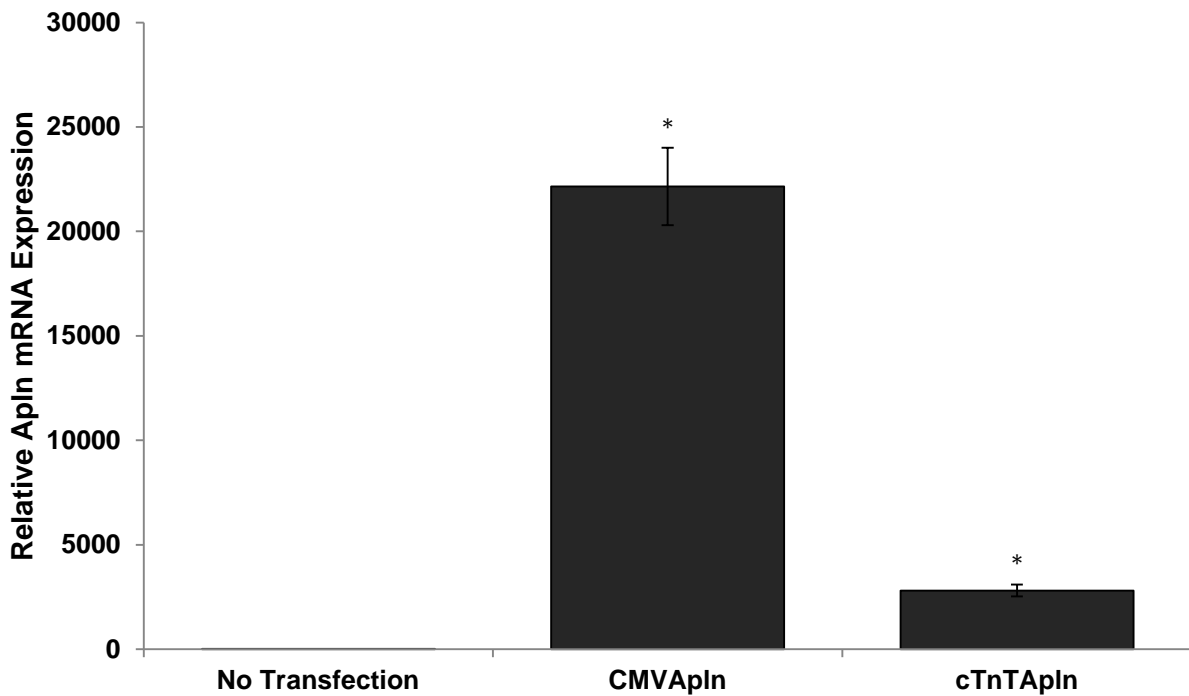
Figure 8. mRNA analysis of AAV-293 cells transfected with pACMVApln, pAcTnTApln, or not transfected and harvested three days post transfection. pAcTnTApln transfected cells show 2800-fold more NRG-1β mRNA expression relative to cells that did not undergo transfection. mRNA expression was normalized to GAPDH. (n=3/group, p<0.01)

Media Conditioned With Apelin Secreted from Transfected 293 Cells Did Not Show Increased Proliferation of bEND.3 Cell Line: To determine if the expression cassettes were producing functional protein, a proliferation assay was performed on the bEND.3 cell line, which expresses the APJ receptor. Compared to media conditioned on pAcTnTGFP-transfected cells, the media conditioned on pAcTnTGFP- and pACMVGFP-transfected cells did not show a significant difference in cell density after three days. All three conditions were highly proliferative, thus, assay conditions must be optimized to bring down basal proliferation in order to see a difference from treatment.

Discussion: While in vitro RNA experiments have shown promise with the pAcTnTApln plasmid, I am unable to show that functional protein is being expressed from transfection with the plasmid. However, I believe this is more down to the assay conditions than presence or absence of functional protein. In short, my assay was not sensitive enough to

34

detect any proliferation beyond the basal bEND.3 proliferation. As all conditions proliferated at approximately the same rate, a lower concentration of serum could be used in the media for the next assay. Alternatively, cells could be treated with a proliferation inhibitor prior to treatment with conditioned media. Immunoblotting with an anti-apelin antibody would also be worthwhile to show the presence of protein, although it would not prove that the protein is indeed functional in causing cell signaling responses upon binding to APJ receptors.

As other studies on the effects of apelin in the heart have recently shown, this protein may hold promise as a therapeutic for heart failure patients. In the previous section I described the design of an AAV2-ITR flanked expression cassette for apelin. However, at this stage, it is too early to comment on its effectiveness beyond its ability to cause an increase in mRNA transcript in vitro. Further in vitro analysis should be performed before this cassette is packaged into AAV and tested in vivo.

Bibliography

1. Go AS, Mozaffarian D, Roger VL, et al. *Heart disease and stroke statistics--2014 update: a report from the American Heart Association.* 2014:e28-e292. doi:10.1161/01.cir.0000441139.02102.80.

2. Cohn JN, Ferrari R, Sharpe N. Cardiac remodeling—concepts and clinical implications: a consensus paper from an international forum on cardiac remodeling. *Journal of the American College of Cardiology*. 2000;35(3):569-582. doi:10.1016/S0735-1097(99)00630-0.

3. White HD, Norris RM, Brown M a., Brandt PW, Whitlock RM, Wild CJ. Left ventricular end-systolic volume as the major determinant of survival after recovery from myocardial infarction. *Circulation*. 1987;76(1):44-51. doi:10.1161/01.CIR.76.1.44.

4. French B A. Post-Infarct LV Remodeling. 2008;4(3):185-196.

5. Ratcliffe MB, Francisco S. Non-Ischemic Infarct Extension * A New Type of Infarct Enlargement and a Potential Therapeutic Target. 2002;40(6).

6. Laflamme M a, Murry CE. Heart regeneration. *Nature*. 2011;473(7347):326-35. doi:10.1038/nature10147.

7. Steinhauser ML, Lee RT. Regeneration of the heart. *EMBO molecular medicine*. 2011;3(12):701-12. doi:10.1002/emmm.201100175.

8. Beltrami AP, Barlucchi L, Torella D, et al. Adult cardiac stem cells are multipotent and support myocardial regeneration. *Cell*. 2003;114(6):763-76. Available at: http://www.ncbi.nlm.nih.gov/pubmed/14505575.

9. Beltrami A, Urbanek K. Evidence that human cardiac myocytes divide after myocardial infarction. *… England Journal of …*. 2001;344(23). Available at: http://www.nejm.org/doi/full/10.1056/NEJM200106073442303. Accessed March 30, 2014.

10. Doppler S a, Deutsch M-A, Lange R, Krane M. Cardiac regeneration: current therapies-future concepts. *Journal of thoracic disease*. 2013;5(5):683-97. doi:10.3978/j.issn.2072-1439.2013.08.71.

11. Ross AJ, Yang Z, Berr SS, et al. Serial MRI evaluation of cardiac structure and function in mice after reperfused myocardial infarction. *Magnetic resonance in medicine : official journal of the Society of Magnetic Resonance in Medicine / Society of Magnetic Resonance in Medicine*. 2002;47(6):1158-68. doi:10.1002/mrm.10166.

12. Konkalmatt P, Wang F, Piras B. Adeno-associated virus serotype 9 administered systemically after reperfusion preferentially targets cardiomyocytes in the infarct border zone with pharmacodynamics. *The journal of gene ….* 2012;(October):609-620. doi:10.1002/jgm.

13. Daya S, Berns KI. Gene therapy using adeno-associated virus vectors. *Clinical microbiology reviews.* 2008;21(4):583-93. doi:10.1128/CMR.00008-08.

14. Hernandez YJ, Wang J, Kearns WG, Loiler S, Poirier A, Flotte TR. Latent Adeno-Associated Virus Infection Elicits Humoral but Not Cell-Mediated Immune Responses in a Nonhuman Primate Model Latent Adeno-Associated Virus Infection Elicits Humoral but Not Cell-Mediated Immune Responses in a Nonhuman Primate Model. 1999.

15. Du L, Kido M, Lee DV, et al. Differential myocardial gene delivery by recombinant serotype-specific adeno-associated viral vectors. *Molecular therapy : the journal of the American Society of Gene Therapy.* 2004;10(3):604-8. doi:10.1016/j.ymthe.2004.06.110.

16. Zincarelli C, Soltys S, Rengo G, Rabinowitz JE. Analysis of AAV serotypes 1-9 mediated gene expression and tropism in mice after systemic injection. *Molecular therapy : the journal of the American Society of Gene Therapy.* 2008;16(6):1073-80. doi:10.1038/mt.2008.76.

17. Prasad KR, Xu Y, Yang Z, Toufektsian M, Berr SS, French BA. Topoisomerase Inhibition Accelerates Gene Expression after Adeno-associated Virus-mediated Gene Transfer to the Mammalian Heart. 2007;15(4):764-771. doi:10.1038/mt.sj.6300071.

18. Inagaki K, Fuess S, Storm T a, et al. Robust systemic transduction with AAV9 vectors in mice: efficient global cardiac gene transfer superior to that of AAV8. *Molecular therapy : the journal of the American Society of Gene Therapy.* 2006;14(1):45-53. doi:10.1016/j.ymthe.2006.03.014.

19. Holmes WE, Mark X, Henzel J, et al. William E. Holmes,* Mark X. 1992;256(May).

20. Meyer D, Birchmeier C. Multiple essential functions of neuregulin in development. *Nature.* 1995;378(6555):386-90. doi:10.1038/378386a0.

21. Lee KF, Simon H, Chen H, Bates B, Hung MC, Hauser C. Requirement for neuregulin receptor erbB2 in neural and cardiac development. *Nature.* 1995;378(6555):394-8. doi:10.1038/378394a0.

22. Gassmann M, Casagranda F, Orioli D, et al. Aberrant neural and cardiac development in mice lacking the ErbB4 neuregulin receptor. *Nature.* 1995;378(6555):390-4. doi:10.1038/378390a0.

23.   Falls D. Neuregulins: functions, forms, and signaling strategies. *Experimental Cell Research*. 2003;284(1):14-30. doi:10.1016/S0014-4827(02)00102-7.

24.   Mei L, Xiong W-C. Neuregulin 1 in neural development, synaptic plasticity and schizophrenia. *Nature reviews Neuroscience*. 2008;9(6):437-52. doi:10.1038/nrn2392.

25.   Odiete O, Hill MF, Sawyer DB. Neuregulin in cardiovascular development and disease. *Circulation research*. 2012;111(10):1376-85. doi:10.1161/CIRCRESAHA.112.267286.

26.   Pentassuglia L, Sawyer DB. The role of Neuregulin-1beta/ErbB signaling in the heart. *Experimental cell research*. 2009;315(4):627-37. doi:10.1016/j.yexcr.2008.08.015.

27.   Luo X, Prior M, He W, et al. Cleavage of neuregulin-1 by BACE1 or ADAM10 protein produces differential effects on myelination. *The Journal of biological chemistry*. 2011;286(27):23967-74. doi:10.1074/jbc.M111.251538.

28.   Fleck D, van Bebber F, Colombo A, et al. Dual cleavage of neuregulin 1 type III by BACE1 and ADAM17 liberates its EGF-like domain and allows paracrine signaling. *The Journal of neuroscience : the official journal of the Society for Neuroscience*. 2013;33(18):7856-69. doi:10.1523/JNEUROSCI.3372-12.2013.

29.   Zhao Y -y. Neuregulins Promote Survival and Growth of Cardiac Myocytes. PERSISTENCE OF ErbB2 AND ErbB4 EXPRESSION IN NEONATAL AND ADULT VENTRICULAR MYOCYTES. *Journal of Biological Chemistry*. 1998;273(17):10261-10269. doi:10.1074/jbc.273.17.10261.

30.   Sawyer DB. Modulation of Anthracycline-Induced Myofibrillar Disarray in Rat Ventricular Myocytes by Neuregulin-1beta and Anti-erbB2: Potential Mechanism for Trastuzumab-Induced Cardiotoxicity. *Circulation*. 2002;105(13):1551-1554. doi:10.1161/01.CIR.0000013839.41224.1C.

31.   Pentassuglia L, Timolati F, Seifriz F, Abudukadier K, Suter TM, Zuppinger C. Inhibition of ErbB2/neuregulin signaling augments paclitaxel-induced cardiotoxicity in adult ventricular myocytes. *Experimental cell research*. 2007;313(8):1588-601. doi:10.1016/j.yexcr.2007.02.007.

32.   Parodi EM, Kuhn B. Signalling between microvascular endothelium and cardiomyocytes through neuregulin. *Cardiovascular research*. 2014;25:1-11. doi:10.1093/cvr/cvu021.

33.   Formiga FR, Pelacho B, Garbayo E, et al. Controlled delivery of fibroblast growth factor-1 and neuregulin-1 from biodegradable microparticles promotes cardiac repair in a rat myocardial infarction model through activation of endogenous regeneration. *Journal of controlled release : official journal of the Controlled Release Society*. 2014;173:132-9. doi:10.1016/j.jconrel.2013.10.034.

34. Bersell K, Arab S, Haring B, Kühn B. Neuregulin1/ErbB4 signaling induces cardiomyocyte proliferation and repair of heart injury. *Cell*. 2009;138(2):257-70. doi:10.1016/j.cell.2009.04.060.

35. Liu X, Gu X, Li Z, et al. Neuregulin-1/erbB-activation improves cardiac function and survival in models of ischemic, dilated, and viral cardiomyopathy. *Journal of the American College of Cardiology*. 2006;48(7):1438-47. doi:10.1016/j.jacc.2006.05.057.

36. Xiao J, Li B, Zheng Z, et al. Therapeutic effects of neuregulin-1 gene transduction in rats with myocardial infarction. *Coronary artery disease*. 2012;23(7):460-8. doi:10.1097/MCA.0b013e32835877da.

37. Liu W, Li J, Roth R a. Heregulin regulation of Akt/protein kinase B in breast cancer cells. *Biochemical and biophysical research communications*. 1999;261(3):897-903. doi:10.1006/bbrc.1999.1144.

38. Levitt N, Briggs D, Gil a, Proudfoot NJ. Definition of an efficient synthetic poly(A) site. *Genes & Development*. 1989;3(7):1019-1025. doi:10.1101/gad.3.7.1019.

39. Tatemoto K, Hosoya M, Habata Y, et al. Isolation and characterization of a novel endogenous peptide ligand for the human APJ receptor. *Biochemical and biophysical research communications*. 1998;251(2):471-6. doi:10.1006/bbrc.1998.9489.

40. Chandrasekaran B, Dar O, McDonagh T. The role of apelin in cardiovascular function and heart failure. *European journal of heart failure*. 2008;10(8):725-32. doi:10.1016/j.ejheart.2008.06.002.

41. Kleinz MJ, Skepper JN, Davenport AP. Immunocytochemical localisation of the apelin receptor, APJ, to human cardiomyocytes, vascular smooth muscle and endothelial cells. *Regulatory peptides*. 2005;126(3):233-40. doi:10.1016/j.regpep.2004.10.019.

42. Japp AG, Newby DE. The apelin-APJ system in heart failure: pathophysiologic relevance and therapeutic potential. *Biochemical pharmacology*. 2008;75(10):1882-92. doi:10.1016/j.bcp.2007.12.015.

43. Tatemoto K, Takayama K, Zou MX, et al. The novel peptide apelin lowers blood pressure via a nitric oxide-dependent mechanism. *Regulatory peptides*. 2001;99(2-3):87-92. Available at: http://www.ncbi.nlm.nih.gov/pubmed/11384769.

44. Chandrasekaran B, Kalra PR, Donovan J, Hooper J, Clague JR, McDonagh T a. Myocardial apelin production is reduced in humans with left ventricular systolic dysfunction. *Journal of cardiac failure*. 2010;16(7):556-61. doi:10.1016/j.cardfail.2010.02.004.

45. Chong KS, Gardner RS, Morton JJ, Ashley E a, McDonagh T a. Plasma concentrations of the novel peptide apelin are decreased in patients with chronic heart failure.

European journal of heart failure. 2006;8(4):355-60. doi:10.1016/j.ejheart.2005.10.007.

46.   Szokodi I. Apelin, the Novel Endogenous Ligand of the Orphan Receptor APJ, Regulates Cardiac Contractility. *Circulation Research*. 2002;91(5):434-440. doi:10.1161/01.RES.0000033522.37861.69.

47.   Tempel D, Boer M, Deel ED, et al. Apelin enhances cardiac neovascularization after myocardial infarction by recruiting aplnr+ circulating cells. *Circulation research*. 2012;111(5):585-98. doi:10.1161/CIRCRESAHA.111.262097.

48.   Ashley E a, Powers J, Chen M, et al. The endogenous peptide apelin potently improves cardiac contractility and reduces cardiac loading in vivo. *Cardiovascular research*. 2005;65(1):73-82. doi:10.1016/j.cardiores.2004.08.018.